JOURNAL OF MATERIALS PROCESSING TECHNOLOGY 206 (2008) 509–510

available at www.sciencedirect.com

ScienceDirect

journal homepage: www.elsevier.com/locate/jmatprotec

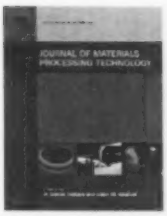

# Author Index of Volume 206

Aboulkas, A., 16
Adeva, P., 99
Aijun, T., 345
Akbarzadeh, A., 92
Aksoy, S., 241
Aksoy, T., 231
Alizadeh, P., 126
Álvarez-Antolín, J.F., 202
Amancio-Filho, S.T., 132
Antolovich, S.D., 30
Arabshahi, H., 25
Arman, Y., 241
Asensio-Lozano, J., 202

Bae, D.-s., 315
Bahrami, A., 126
Bai, C., 382
Bai, H.B., 412
Bathias, C., 30
Bayraktar, E., 30
Beltrão, P.A.C., 184
Bhaduri, S.B., 221
Bolandi, M., 126
Bolfarini, C., 132
Borges, P.C., 184
Burakorn, T., 352

Cavaliere, P., 249
Çelik, E., 241
Chaisuk, C., 352
Chandradass, J., 315
Chen, C.-C., 425
Cheng, C.-H., 491
Cheng, J.P., 180
Cheng, Y., 445
Chiu, C.-H., 419
Çiçek, A., 106
Cioffi, N., 462
Culha, O., 231

Daneshi, G.H., 92
De Tiedra, P., 256
Demirci, H.İ., 152
Di Franco, C., 462
Diau, E.W.-G., 425
Diniz, A.E., 294
Ditaranto, N., 462
dos Santos, J.F., 132

Ebrahimi, G.R., 25
El bouadili, A., 16
El harfi, K., 16
El-Tayeb, N.S.M., 305
Enying, L., 45

Esner, C., 152
Eto, A.M., 184

Ferrer, J.A.G., 294
Firouzdor, V., 467
Fusheng, P., 374

Gao, Z.-W., 419
Garcés, G., 99
Ger, M.-D., 56
Gologlu, C., 7
Gomes, C.M., 194
Grandhi, R.V., 263
Grangure, P., 328
Greil, P., 194
Guo, E.J., 161
Guoxin, H., 395

Haghshenas, M., 25
Hajipour, A., 62
Han, F., 328
Han, K.-S., 315
Hasçiçek, Y.S., 241
Hatakeyama, M., 322
He, Z.-B., 400
Heidarbeigy, M., 388
Hotza, D., 194
Hou, J.F., 412
Hu, W., 45
Huo, Y.L., 500
Hwang, I.C., 69, 143
Hwang, L.-R., 491
Hwu, W.-H., 56

Imahori, S., 453
Ismail, M.M., 83

Jain, P.K., 167
Jongsomjit, B., 352
Juan, M.S., 256

Karimzadeh, F., 388
Kermanpur, A., 62
Khameneh Asl, Sh., 92
Khodai, M., 1
Khomamizadeh, F., 467
Kunieda, M., 328
Kushiya, M., 453

Lalwani, D.I., 167
Leong, K.H., 120
Li, D.W., 412
Li, J.S., 445
Li, Y., 365

Li, Y.P., 431
Liang, B., 374
Liao, R.H., 445
Lin, H.-W., 56
Lin, J.-S., 425
Lin, Y.-C., 491
Liu, N., 365
Liu, T.-F., 425
Lixiang, Z., 395
López, M., 256
Lou, S., 481

Ma, B.X., 161
Maciejewski, J., 333
Mahmoudi, S., 62
Malik, A.S., 263
Marcondes, P.V.P., 184
Martín, Ó., 256
Mehta, N.K., 167
Mekasuwandumrong, O., 352
Mingbo, Y., 374
Mróz, Z., 333
Müller, A., 99

Naghizadeh, R., 282
Nakashima, T., 453
Nejati, E., 467
Nemati, Z.A., 126
Ng, S.-P., 359

Okumiya, M., 322
Oliveira, A.P.N., 194
Oñorbe, E., 99

Pan, F., 382
Panella, F., 249
Panpranot, J., 352
Park, C.J., 69, 143
Parvin, N., 1
Pérez, P., 99
Platts, M.J., 78
Praserthdam, P., 352

Rajendran, R., 275
Ramesh, Sh., 221
Rasouli, D., 92
Reed, C.B., 120
Ren, C.-S., 216
Ren, L.-q., 473
Renju, C., 374
Rezaie, H.R., 282
Rong, C., 365
Ruan, F., 500

Elsevier B.V.
doi:10.1016/S0924-0136(08)00483-4

Saatchi, A., 388
Sahin, S., 231
Sakarya, N., 7
Sayman, O., 241
Scamarcio, G., 462
Sheikhi, S., 132
Sheriff, N.M., 83
Shi, L., 438
Sibilano, M., 462
Singh, R., 286
Sobhani, M., 282
Sopyan, I., 221
Su, P.-L., 491
Sugihara, K., 453
Sun, X.Y., 445

Tamura, S., 322
Tan, C.Y., 221
Tang, J.G., 431
Teng, W.D., 221
Tong, X., 473
Toparli, M., 231
Torsi, L., 462
Travitzky, N., 194
Tsao, C.C., 405
Tsunekawa, Y., 322

Vitiello, M.S., 462
Voort, G.F.V., 202

Wang, D.-Z., 216
Wang, L.J., 445
Wang, L.P., 161
Wang, R., 481
Wang, T., 78
Wang, Y.-N., 216
Wang, Z.R., 400
Wei, Z., 438
Wu, H.-Y., 419
Wu, J., 78
Wu, X., 481

Xi, M., 438
Xia, Q.X., 500
Xie, S.W., 500
Xu, Z., 120

Yanhong, L., 395
Yao, L.G., 45
Yasar, M., 152
Ye, Y., 180
Yip, J., 359
Yuan, S.-J., 400
Yunliang, F., 395

Zarei-Hanzaki, A., 25
Zhang, J., 382
Zhang, W., 473
Zhang, X., 365
Zhang, X.B., 180
Zhang, Y., 438
Zhang, Z.-h., 473
Zhanqiang, L., 345
Zhao, G., 481
Zhou, G.-Z., 419
Zhou, H., 473
Zhou, L.Q., 431
Zhou, Y.C., 431
Zuo, R., 382

JOURNAL OF MATERIALS PROCESSING TECHNOLOGY 206 (2008) 511–518

available at www.sciencedirect.com

ScienceDirect

journal homepage: www.elsevier.com/locate/jmatprotec

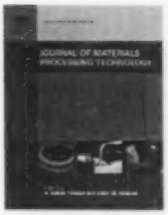

# Subject Index of Volume 206

AA5754-O
Effect of the blank holder force on drawing of aluminum alloy square cup: Theoretical and experimental investigation, 152
AAO
Fabrication and characterization of eutectic gold–silicon (Au–Si) nanowires, 425
2B abrasion wear
Abrasive wear performance of untreated SCF reinforced polymer composite, 305
Acicular ferrite
Effect of cooling rate on the microstructure and mechanical properties of microalloyed forging steel, 92
Activation energy
Kinetic and mechanism of Tarfaya (Morocco) oil shale and LDPE mixture pyrolysis, 16
Adjacency relation matrix
Similarity and scaling assessments of mechanical parts using adjacency relation matrices, 106
Aircraft
Preliminary study on the microstructure and mechanical properties of dissimilar friction stir welds in aircraft aluminium alloys 2024-T351 and 6056-T4, 132
Al 2024
The effect of heat treatment on hot deformation behaviour of Al 2024, 25
Alloy indefinite chill
Identification and quantification of active manufacturing factors for graphite formation in centrifugally cast Nihard cast irons, 202
Alumina
Characterization of cobalt dispersed on the mixed nanoscale alumina and zirconia supports, 352
Aluminium
Preliminary study on the microstructure and mechanical properties of dissimilar friction stir welds in aircraft aluminium alloys 2024-T351 and 6056-T4, 132
Aluminium foil
The low temperature precipitation in commercial-purity aluminium sheets for foils, 382
Aluminum alloy extrusion
Modeling of aluminum alloy profile extrusion process using finite volume method, 481
Aluminum titanate
Sol–gel synthesis of aluminum titanate ($Al_2TiO_5$) nanoparticles, 282
Analysis of variance
Investigation into the effects of drilling parameters on delamination by various step-core drills, 405
Anisotropy
Mechanical properties and formability of an Mg–6%Li–1%Zn alloy thin sheet at elevated temperatures, 419
Anisotropy constant
Predicting forming limit of electrodeposited nickel coating based on practical stress–strain relationship, 431
Annealing
The low temperature precipitation in commercial-purity aluminium sheets for foils, 382
Artificial neural networks
Prediction of magnetic interference from resistance spot welding processes on implantable cardioverter-defibrillators, 256
Au–Si alloy
Fabrication and characterization of eutectic gold–silicon (Au–Si) nanowires, 425
Automatic width control
Width control systems with roll force automatic width control and finishing vertical mill automatic width control in hot strip mill, 143
Automotive components
Numerical simulation of metal flow and solidification in the multi-cavity casting moulds of automotive components, 62

Bending strength
Effects of electrical discharge energy on machining performance and bending strength of cemented tungsten carbides, 491
Bioceramic
Densification behaviour of nanocrystalline hydroxyapatite bioceramics, 221
Biomimetic
Thermal fatigue behavior of gray cast iron with striated biomimetic non-smooth surface, 473
Bismuth
Modification of $Mg_2Si$ morphology in Mg–Si alloys with Bi, 161
Boride layers
Characterization and determination of $Fe_xB$ layers' mechanical properties, 231
Boundary and best neighbor sampling (BBNS)
Optimization of drawbead design in sheet metal forming based on intelligent sampling by using response surface methodology, 45

Elsevier B.V.
doi:10.1016/S0924-0136(08)00484-6

Broaching
A smart stamping tool for punching and broaching combination, 184

Carbide precipitation
Effect of deep cryogenic treatment on wear resistance and tool life of M2 HSS drill, 467
Carbide tool
A comparison between silicon nitride-based ceramic and coated carbide tools in the face milling of irregular surfaces, 294
Carbon content
Effect of carbon content on the microstructure and mechanical properties of ultra-fine grade (Ti,W)(C,N)-Co cermets, 365
Carbon nanotubes
Reduction process of nickel cations anchored on carbon nanotubes, 180
Casting
Numerical simulation of metal flow and solidification in the multi-cavity casting moulds of automotive components, 62
Catalyst
Characterization of cobalt dispersed on the mixed nanoscale alumina and zirconia supports, 352
Cemented tungsten carbide
Effects of electrical discharge energy on machining performance and bending strength of cemented tungsten carbides, 491
Centrifugal casting
Identification and quantification of active manufacturing factors for graphite formation in centrifugally cast Nihard cast irons, 202
Circular plates
Reloading effects on plane plates subjected to non-contact underwater explosion, 275
Coating sheet
Predicting forming limit of electrodeposited nickel coating based on practical stress–strain relationship, 431
Cobalt
Characterization of cobalt dispersed on the mixed nanoscale alumina and zirconia supports, 352
Composite materials
New developments in non-destructive controls of the composite materials and applications in manufacturing engineering, 30
Composites
Characterization of laser powder deposited Ti–TiC composites and functional gradient materials, 438
Cooling rate
Effect of cooling rate on the microstructure and mechanical properties of microalloyed forging steel, 92
Corrosion
Effect of heat treatment on corrosion behavior of Ti–6Al–4V alloy weldments, 388
Crack
Thermal fatigue behavior of gray cast iron with striated biomimetic non-smooth surface, 473
Crack behaviour
Effect of tool position on the fatigue properties of dissimilar 2024-7075 sheets joined by friction stir welding, 249
Crown
A computational method to predict strip profile in rolling mills, 263

Cryogenic treatment
Effect of deep cryogenic treatment on wear resistance and tool life of M2 HSS drill, 467
Crystallization
Crystallization and electrical properties of $[(Pb_{1-x}Sr_x)\cdot TiO_3][(2SiO_2\cdot B_2O_3)][K_2O]$ glass–ceramics, 126
Cutter path
Generation of cutter paths for hard material in wire EDM, 453
Cutter path strategies
The effects of cutter path strategies on surface roughness of pocket milling of 1.2738 steel based on Taguchi method, 7
Cutting forces
Experimental investigations of cutting parameters influence on cutting forces and surface roughness in finish hard turning of MDN250 steel, 167
Cyclic torsion
An upper-bound analysis of axisymmetric extrusion assisted by cyclic torsion, 333

Damage mechanism
New developments in non-destructive controls of the composite materials and applications in manufacturing engineering, 30
Damping capacity measurement method
Damping capacity measurement of elastic porous wire-mesh material in wide temperature range, 412
Damping material
Damping capacity measurement of elastic porous wire-mesh material in wide temperature range, 412
DBD
Improvement of the graft and dyeability of linen by DBD treatment in ambient air, 216
Deformations
Influence of cold rolling on sensitization and intergranular stress corrosion cracking of AISI 304 aged at 500 °C, 286
Deformations of thin-walled plate due to static end milling force, 345
Deformation of revolving closed-shell with multi-curvature profile under inner pressure, 400
Degradation mechanism
Kinetic and mechanism of Tarfaya (Morocco) oil shale and LDPE mixture pyrolysis, 16
Degree of sensitization
Influence of cold rolling on sensitization and intergranular stress corrosion cracking of AISI 304 aged at 500 °C, 286
Delamination
Investigation into the effects of drilling parameters on delamination by various step-core drills, 405
Die-casting
Fabrication and characterization of eutectic gold–silicon (Au–Si) nanowires, 425
Dielectric properties
Crystallization and electrical properties of $[(Pb_{1-x}Sr_x)\cdot TiO_3][(2SiO_2\cdot B_2O_3)][K_2O]$ glass–ceramics, 126
Diffusion
Effect of deep cryogenic treatment on wear resistance and tool life of M2 HSS drill, 467
Discharge location
Improvement in accuracy in potential method for detecting EDM spark locations, 328

Discharge noise
Improvement in accuracy in potential method for detecting EDM spark locations, 328
Dispersion
The dispersion of silver nanoparticles with physical dispersal procedures, 56
Dissimilar joints
Preliminary study on the microstructure and mechanical properties of dissimilar friction stir welds in aircraft aluminium alloys 2024-T351 and 6056-T4, 132
Drawbead
Optimization of drawbead design in sheet metal forming based on intelligent sampling by using response surface methodology, 45
Numerical design optimisation of drawbead position and experimental validation of cup drawing process, 83
Drilling
Investigation into the effects of drilling parameters on delamination by various step-core drills, 405
DTA
Crystallization and electrical properties of $[(Pb_{1-x}Sr_x)\cdot TiO_3][(2SiO_2\cdot B_2O_3)][K_2O]$ glass–ceramics, 126
Duplex rolls
Identification and quantification of active manufacturing factors for graphite formation in centrifugally cast Nihard cast irons, 202
Dyeability
Improvement of the graft and dyeability of linen by DBD treatment in ambient air, 216
DYNAFORM
Numerical design optimisation of drawbead position and experimental validation of cup drawing process, 83
Dynamic recovery
The effect of heat treatment on hot deformation behaviour of Al 2024, 25

Earings
Effect of the blank holder force on drawing of aluminum alloy square cup: Theoretical and experimental investigation, 152
EDM
Improvement in accuracy in potential method for detecting EDM spark locations, 328
Effects of electrical discharge energy on machining performance and bending strength of cemented tungsten carbides, 491
Elastic modulus
Characterization and determination of $Fe_xB$ layers' mechanical properties, 231
Electrodeposited nickel coating
Predicting forming limit of electrodeposited nickel coating based on practical stress–strain relationship, 431
End milling
The effects of cutter path strategies on surface roughness of pocket milling of 1.2738 steel based on Taguchi method, 7
Deformations of thin-walled plate due to static end milling force, 345
Eutectic nanowire
Fabrication and characterization of eutectic gold–silicon (Au–Si) nanowires, 425
Extrusion
An upper-bound analysis of axisymmetric extrusion assisted by cyclic torsion, 333

Factorial design
LZSA glass-ceramic laminates: Fabrication and mechanical properties, 194
Fatigue
Effect of tool position on the fatigue properties of dissimilar 2024-7075 sheets joined by friction stir welding, 249
Feedback AWC
Width control systems with roll force automatic width control and finishing vertical mill automatic width control in hot strip mill, 143
Ferrous alloys
Nondestructive evaluation and real-time monitoring of laser surface hardening, 120
Finish hard turning
Experimental investigations of cutting parameters influence on cutting forces and surface roughness in finish hard turning of MDN250 steel, 167
Finishing mill
Width control systems with roll force automatic width control and finishing vertical mill automatic width control in hot strip mill, 143
Finite element analysis (FEA)
The optimisation of shot peen forming processes, 78
Finite element analyze
Effect of the blank holder force on drawing of aluminum alloy square cup: Theoretical and experimental investigation, 152
Finite volume method
Numerical simulation of metal flow and solidification in the multi-cavity casting moulds of automotive components, 62
Modeling of aluminum alloy profile extrusion process using finite volume method, 481
Fischer-Tropsch synthesis
Characterization of cobalt dispersed on the mixed nanoscale alumina and zirconia supports, 352
Flatness
A computational method to predict strip profile in rolling mills, 263
Force-support tree
Generation of cutter paths for hard material in wire EDM, 453
Formability parameter
Mechanical properties and formability of an Mg–6%Li–1%Zn alloy thin sheet at elevated temperatures, 419
Forming limit diagram
Mechanical properties and formability of an Mg–6%Li–1%Zn alloy thin sheet at elevated temperatures, 419
Predicting forming limit of electrodeposited nickel coating based on practical stress–strain relationship, 431
Fourier transform infrared spectroscopy
Synthesis and characterization of zirconia- and silica-doped zirconia nanopowders by oxalate processing, 315
Fractional Design of Experiments (DOE)
Identification and quantification of active manufacturing factors for graphite formation in centrifugally cast Nihard cast irons, 202

Fracture toughness
Characterization and determination of $Fe_xB$ layers' mechanical properties, 231
Friction stir welding
Preliminary study on the microstructure and mechanical properties of dissimilar friction stir welds in aircraft aluminium alloys 2024-T351 and 6056-T4, 132
FSW
Effect of tool position on the fatigue properties of dissimilar 2024-7075 sheets joined by friction stir welding, 249
Functional gradient materials
Characterization of laser powder deposited Ti–TiC composites and functional gradient materials, 438

Glass ceramics
Crystallization and electrical properties of $[(Pb_{1-x}Sr_x)\cdot TiO_3][(2SiO_2\cdot B_2O_3)][K_2O]$ glass–ceramics, 126
LZSA glass-ceramic laminates: Fabrication and mechanical properties, 194
Graft
Improvement of the graft and dyeability of linen by DBD treatment in ambient air, 216
Graphite
Identification and quantification of active manufacturing factors for graphite formation in centrifugally cast Nihard cast irons, 202
Gray casting iron
A comparison between silicon nitride-based ceramic and coated carbide tools in the face milling of irregular surfaces, 294
Thermal fatigue behavior of gray cast iron with striated biomimetic non-smooth surface, 473

Hardness
Characterization and determination of $Fe_xB$ layers' mechanical properties, 231
Characterization of laser powder deposited Ti–TiC composites and functional gradient materials, 438
Head of strip
New tension control at the head of strip in hot strip finishing mill, 69
Heat treatment
The effect of heat treatment on hot deformation behaviour of Al 2024, 25
Effect of heat treatment on corrosion behavior of Ti–6Al–4V alloy weldments, 388
High–low temperature
Damping capacity measurement of elastic porous wire-mesh material in wide temperature range, 412
High-speed dry drilling
Effect of deep cryogenic treatment on wear resistance and tool life of M2 HSS drill, 467
Hole making
A smart stamping tool for punching and broaching combination, 184
Hot deformation
The effect of heat treatment on hot deformation behaviour of Al 2024, 25
Hot forging
Effect of hot forging on the microstructure and mechanical properties of Mg–Zn–Y alloy, 99
Hot strip finishing mill
New tension control at the head of strip in hot strip finishing mill, 69
Hot strip mill
Width control systems with roll force automatic width control and finishing vertical mill automatic width control in hot strip mill, 143
Hydroforming
Deformation of revolving closed-shell with multi-curvature profile under inner pressure, 400
Hydroxyapatite
Densification behaviour of nanocrystalline hydroxyapatite bioceramics, 221
Hysteresis loop
Damping capacity measurement of elastic porous wire-mesh material in wide temperature range, 412

Icosahedral quasicrystalline phase
Effect of hot forging on the microstructure and mechanical properties of Mg–Zn–Y alloy, 99
Implantable cardioverter-defibrillator
Prediction of magnetic interference from resistance spot welding processes on implantable cardioverter-defibrillators, 256
Industrial constraints
Generation of cutter paths for hard material in wire EDM, 453
Infrared sensors
Nondestructive evaluation and real-time monitoring of laser surface hardening, 120
Insulation
The effect on residual stresses of porosity and surface roughness in high temperature insulation coatings on Ag tape for magnet technologies, 241
Interface
Characterization of laser powder deposited Ti–TiC composites and functional gradient materials, 438
Intergranular stress corrosion cracking
Influence of cold rolling on sensitization and intergranular stress corrosion cracking of AISI 304 aged at 500 °C, 286

KOBO method
An upper-bound analysis of axisymmetric extrusion assisted by cyclic torsion, 333

Laser powder deposition
Characterization of laser powder deposited Ti–TiC composites and functional gradient materials, 438
Laser surface hardening
Nondestructive evaluation and real-time monitoring of laser surface hardening, 120
Linen
Improvement of the graft and dyeability of linen by DBD treatment in ambient air, 216
Looper system
New tension control at the head of strip in hot strip finishing mill, 69
Lost foam casting
Pressure measurement and some observation in lost foam casting, 1
Low-density polyethylene (LDPE)
Kinetic and mechanism of Tarfaya (Morocco) oil shale and LDPE mixture pyrolysis, 16

M2 high-speed steel drill
Effect of deep cryogenic treatment on wear resistance and tool life of M2 HSS drill, 467
Machines
Synthesis research of nanosized ZSM-5 zeolites in the absence of organic template, 445

Magnesium
Modification of $Mg_2Si$ morphology in Mg–Si alloys with Bi, 161
Magnesium alloy
Effect of hot forging on the microstructure and mechanical properties of Mg–Zn–Y alloy, 99
Magnesium–lithium alloy
Mechanical properties and formability of an Mg–6%Li–1%Zn alloy thin sheet at elevated temperatures, 419
Magnetic fields
Prediction of magnetic interference from resistance spot welding processes on implantable cardioverter-defibrillators, 256
Main motor current
New tension control at the head of strip in hot strip finishing mill, 69
Maraging steel
Experimental investigations of cutting parameters influence on cutting forces and surface roughness in finish hard turning of MDN250 steel, 167
MARC
Numerical simulation and experimental research on the multi-pass neck-spinning of non-axisymmetric offset tube, 500
Material removal rate
Effects of electrical discharge energy on machining performance and bending strength of cemented tungsten carbides, 491
Mathematical model
A computational method to predict strip profile in rolling mills, 263
Mechanical properties
Densification behaviour of nanocrystalline hydroxyapatite bioceramics, 221
Abrasive wear performance of untreated SCF reinforced polymer composite, 305
Study of three-dimensional spacer fabrics:. Physical and mechanical properties, 359
Effect of carbon content on the microstructure and mechanical properties of ultra-fine grade (Ti,W)(C,N)-Co cermets, 365
Metallic glass
Ultrasonic cavitation treatment for soldering on Zr-based bulk metallic glass, 322
Mg–A1–Si-based alloys
Effect of semi-solid isothermal heat treatment on the microstructure of Mg–6A1–1Zn–0.7Si alloy, 374
$Mg_2Si$
Modification of $Mg_2Si$ morphology in Mg–Si alloys with Bi, 161
$Mg_2Si$ phase
Effect of semi-solid isothermal heat treatment on the microstructure of Mg–6A1–1Zn–0.7Si alloy, 374
Microalloyed forging steels
Effect of cooling rate on the microstructure and mechanical properties of microalloyed forging steel, 92
Microstructure
Preliminary study on the microstructure and mechanical properties of dissimilar friction stir welds in aircraft aluminium alloys 2024-T351 and 6056-T4, 132
Modification of $Mg_2Si$ morphology in Mg–Si alloys with Bi, 161
Reduction process of nickel cations anchored on carbon nanotubes, 180
Effect of carbon content on the microstructure and mechanical properties of ultra-fine grade (Ti,W)(C,N)-Co cermets, 365
The low temperature precipitation in commercial-purity aluminium sheets for foils, 382
Characterization of laser powder deposited Ti–TiC composites and functional gradient materials, 438
Milling of irregular surfaces
A comparison between silicon nitride-based ceramic and coated carbide tools in the face milling of irregular surfaces, 294
MIM
Fabrication of high porous NiTi shape memory alloy by metal injection molding, 395
Modification
Modification of $Mg_2Si$ morphology in Mg–Si alloys with Bi, 161
Mold filling
Pressure measurement and some observation in lost foam casting, 1
Moving grids system
Modeling of aluminum alloy profile extrusion process using finite volume method, 481
Multi-curvature
Deformation of revolving closed-shell with multi-curvature profile under inner pressure, 400
Multi-pass spinning
Numerical simulation and experimental research on the multi-pass neck-spinning of non-axisymmetric offset tube, 500

Nanomaterial
Characterization of cobalt dispersed on the mixed nanoscale alumina and zirconia supports, 352
Nanoparticles
The dispersion of silver nanoparticles with physical dispersal procedures, 56
Sol–gel synthesis of aluminum titanate ($Al_2TiO_5$) nanoparticles, 282
Nanosized ZSM-5 zeolite
Synthesis research of nanosized ZSM-5 zeolites in the absence of organic template, 445
Neck-spinning
Numerical simulation and experimental research on the multi-pass neck-spinning of non-axisymmetric offset tube, 500
Nihard cast iron
Identification and quantification of active manufacturing factors for graphite formation in centrifugally cast Nihard cast irons, 202
Non-destructive test
New developments in non-destructive controls of the composite materials and applications in manufacturing engineering, 30
Non-smooth surface
Thermal fatigue behavior of gray cast iron with striated biomimetic non-smooth surface, 473
Numerical simulation
Numerical simulation of metal flow and solidification in the multi-cavity casting moulds of automotive components, 62
Numerical simulation and experimental research on the multi-pass neck-spinning of non-axisymmetric offset tube, 500

Offset tube
Numerical simulation and experimental research on the multi-pass neck-spinning of non-axisymmetric offset tube, 500
Oil shale
Kinetic and mechanism of Tarfaya (Morocco) oil shale and LDPE mixture pyrolysis, 16

One step forming
Optimization of drawbead design in sheet metal forming based on intelligent sampling by using response surface methodology, 45
Optimisation
The optimisation of shot peen forming processes, 78
Optimum
Numerical design optimisation of drawbead position and experimental validation of cup drawing process, 83

Pb-free solder
Ultrasonic cavitation treatment for soldering on Zr-based bulk metallic glass, 322
PCD
Generation of cutter paths for hard material in wire EDM, 453
Photography technique
Pressure measurement and some observation in lost foam casting, 1
Physical properties
Study of three-dimensional spacer fabrics:. Physical and mechanical properties, 359
Plasma activation
Plasma treatment effects on Si and Si/dielectric film heterostructures, 462
Plasma-enhanced chemical vapour deposition
Plasma treatment effects on Si and Si/dielectric film heterostructures, 462
Plastic deformation
Reloading effects on plane plates subjected to non-contact underwater explosion, 275
Polymer
Abrasive wear performance of untreated SCF reinforced polymer composite, 305
Polythionic acid
Influence of cold rolling on sensitization and intergranular stress corrosion cracking of AISI 304 aged at 500 °C, 286
Porosity
The effect on residual stresses of porosity and surface roughness in high temperature insulation coatings on Ag tape for magnet technologies, 241
Porous
Fabrication of high porous NiTi shape memory alloy by metal injection molding, 395
Porous material
Damping capacity measurement of elastic porous wire-mesh material in wide temperature range, 412
Potential method
Improvement in accuracy in potential method for detecting EDM spark locations, 328
Precipitation
The effect of heat treatment on hot deformation behaviour of Al 2024, 25
The low temperature precipitation in commercial-purity aluminium sheets for foils, 382
Primary pulse
Reloading effects on plane plates subjected to non-contact underwater explosion, 275
Process control parameters
An upper-bound analysis of axisymmetric extrusion assisted by cyclic torsion, 333
Process model
The optimisation of shot peen forming processes, 78
Process monitoring
Nondestructive evaluation and real-time monitoring of laser surface hardening, 120
Punching
A smart stamping tool for punching and broaching combination, 184

Quantitative metallography
Identification and quantification of active manufacturing factors for graphite formation in centrifugally cast Nihard cast irons, 202

Rapid prototyping
LZSA glass-ceramic laminates: Fabrication and mechanical properties, 194
Rectangular plates
Reloading effects on plane plates subjected to non-contact underwater explosion, 275
Reloading
Reloading effects on plane plates subjected to non-contact underwater explosion, 275
Resistance spot welding
Prediction of magnetic interference from resistance spot welding processes on implantable cardioverter-defibrillators, 256
Response surface methodology (RSM)
Optimization of drawbead design in sheet metal forming based on intelligent sampling by using response surface methodology, 45
Revolving closed-shell
Deformation of revolving closed-shell with multi-curvature profile under inner pressure, 400
Roll force AWC
Width control systems with roll force automatic width control and finishing vertical mill automatic width control in hot strip mill, 143
Rolling
The low temperature precipitation in commercial-purity aluminium sheets for foils, 382
Rolling mill
A computational method to predict strip profile in rolling mills, 263
Roughing mill
Width control systems with roll force automatic width control and finishing vertical mill automatic width control in hot strip mill, 143

SEM
Abrasive wear performance of untreated SCF reinforced polymer composite, 305
Fabrication of high porous NiTi shape memory alloy by metal injection molding, 395
Semi-solid
Effect of semi-solid isothermal heat treatment on the microstructure of Mg–6A1–1Zn–0.7Si alloy, 374
Semi-solid isothermal heat treatment
Effect of semi-solid isothermal heat treatment on the microstructure of Mg–6A1–1Zn–0.7Si alloy, 374
Sheet forming
Optimization of drawbead design in sheet metal forming based on intelligent sampling by using response surface methodology, 45
Sheet metal forming
Numerical design optimisation of drawbead position and experimental validation of cup drawing process, 83
(Shot) peen forming
The optimisation of shot peen forming processes, 78
Shot peening
The optimisation of shot peen forming processes, 78

Silicon dioxide
Plasma treatment effects on Si and Si/dielectric film heterostructures, 462
Silicon nitride
Plasma treatment effects on Si and Si/dielectric film heterostructures, 462
Silicon nitride-based ceramic
A comparison between silicon nitride-based ceramic and coated carbide tools in the face milling of irregular surfaces, 294
Similarity and scaling assessments
Similarity and scaling assessments of mechanical parts using adjacency relation matrices, 106
SIMPLE algorithm
Modeling of aluminum alloy profile extrusion process using finite volume method, 481
Sintering
Densification behaviour of nanocrystalline hydroxyapatite bioceramics, 221
SMA
Fabrication of high porous NiTi shape memory alloy by metal injection molding, 395
Soldering
Ultrasonic cavitation treatment for soldering on Zr-based bulk metallic glass, 322
Sol–gel
The effect on residual stresses of porosity and surface roughness in high temperature insulation coatings on Ag tape for magnet technologies, 241
Sol–gel synthesis
Sol–gel synthesis of aluminum titanate ($Al_2TiO_5$) nanoparticles, 282
Solid solubility
The low temperature precipitation in commercial-purity aluminium sheets for foils, 382
Solid state reactions
Reduction process of nickel cations anchored on carbon nanotubes, 180
Solidification
Numerical simulation of metal flow and solidification in the multi-cavity casting moulds of automotive components, 62
Sono-capillary effect
Ultrasonic cavitation treatment for soldering on Zr-based bulk metallic glass, 322
Spacer fabrics
Study of three-dimensional spacer fabrics:. Physical and mechanical properties, 359
Square deep drawing
Effect of the blank holder force on drawing of aluminum alloy square cup: Theoretical and experimental investigation, 152
Stainless steels 304
Influence of cold rolling on sensitization and intergranular stress corrosion cracking of AISI 304 aged at 500 °C, 286
STEP
Similarity and scaling assessments of mechanical parts using adjacency relation matrices, 106
Step-core drill
Investigation into the effects of drilling parameters on delamination by various step-core drills, 405
Stress–strain relationship
Predicting forming limit of electrodeposited nickel coating based on practical stress–strain relationship, 431
Striated
Thermal fatigue behavior of gray cast iron with striated biomimetic non-smooth surface, 473
Strip profile
A computational method to predict strip profile in rolling mills, 263
Surface roughness
The effects of cutter path strategies on surface roughness of pocket milling of 1.2738 steel based on Taguchi method, 7
Experimental investigations of cutting parameters influence on cutting forces and surface roughness in finish hard turning of MDN250 steel, 167
The effect on residual stresses of porosity and surface roughness in high temperature insulation coatings on Ag tape for magnet technologies, 241
A comparison between silicon nitride-based ceramic and coated carbide tools in the face milling of irregular surfaces, 294
Effects of electrical discharge energy on machining performance and bending strength of cemented tungsten carbides, 491
Synthesis
Synthesis research of nanosized ZSM-5 zeolites in the absence of organic template, 445

Taguchi method
The effects of cutter path strategies on surface roughness of pocket milling of 1.2738 steel based on Taguchi method, 7
Tape casting
LZSA glass-ceramic laminates: Fabrication and mechanical properties, 194
Tension calculation
New tension control at the head of strip in hot strip finishing mill, 69
Tension control
New tension control at the head of strip in hot strip finishing mill, 69
Thermal degradation
Kinetic and mechanism of Tarfaya (Morocco) oil shale and LDPE mixture pyrolysis, 16
Thermal fatigue
Thermal fatigue behavior of gray cast iron with striated biomimetic non-smooth surface, 473
Thermal stress
The effect on residual stresses of porosity and surface roughness in high temperature insulation coatings on Ag tape for magnet technologies, 241
Thermogravimetric analysis
Kinetic and mechanism of Tarfaya (Morocco) oil shale and LDPE mixture pyrolysis, 16
Thick sheets
A smart stamping tool for punching and broaching combination, 184
Thin-walled plate
Deformations of thin-walled plate due to static end milling force, 345
Thixotropic characteristic
The dispersion of silver nanoparticles with physical dispersal procedures, 56
Three-roller mill
The dispersion of silver nanoparticles with physical dispersal procedures, 56
Ti–6Al–4V alloy
Effect of heat treatment on corrosion behavior of Ti–6Al–4V alloy weldments, 388
(Ti,W) (C,N)-Co cermet
Effect of carbon content on the microstructure and mechanical properties of ultra-fine grade (Ti,W) (C,N)-Co cermets, 365

Tool wear
A comparison between silicon nitride-based ceramic and coated carbide tools in the face milling of irregular surfaces, 294
Toughness
Effect of cooling rate on the microstructure and mechanical properties of microalloyed forging steel, 92
Transmission electron microscopy
Reduction process of nickel cations anchored on carbon nanotubes, 180
Synthesis and characterization of zirconia- and silica-doped zirconia nanopowders by oxalate processing, 315
Synthesis research of nanosized ZSM-5 zeolites in the absence of organic template, 445

Ultrasonic cavitation
Ultrasonic cavitation treatment for soldering on Zr-based bulk metallic glass, 322
Underwater explosion
Reloading effects on plane plates subjected to non-contact underwater explosion, 275
Untreated sugarcane fibre
Abrasive wear performance of untreated SCF reinforced polymer composite, 305
Upper-bound analysis
An upper-bound analysis of axisymmetric extrusion assisted by cyclic torsion, 333

Vacuum smelting
Fabrication and characterization of eutectic gold–silicon (Au–Si) nanowires, 425
Viscosity
The dispersion of silver nanoparticles with physical dispersal procedures, 56
Volume of fluid
Modeling of aluminum alloy profile extrusion process using finite volume method, 481

Wear resistance
Effect of deep cryogenic treatment on wear resistance and tool life of M2 HSS drill, 467
Welding
Preliminary study on the microstructure and mechanical properties of dissimilar friction stir welds in aircraft aluminium alloys 2024-T351 and 6056-T4, 132
Effect of heat treatment on corrosion behavior of Ti–6Al–4V alloy weldments, 388
Width shrinkage
New tension control at the head of strip in hot strip finishing mill, 69
Wire EDM
Generation of cutter paths for hard material in wire EDM, 453
Wire-mesh
Damping capacity measurement of elastic porous wire-mesh material in wide temperature range, 412
Wrinkling
Numerical design optimisation of drawbead position and experimental validation of cup drawing process, 83

X-ray computed tomography medical scanner
New developments in non-destructive controls of the composite materials and applications in manufacturing engineering, 30
X-ray diffraction
Synthesis and characterization of zirconia- and silica-doped zirconia nanopowders by oxalate processing, 315
X-ray techniques
Synthesis research of nanosized ZSM-5 zeolites in the absence of organic template, 445
XRD
Fabrication of high porous NiTi shape memory alloy by metal injection molding, 395

Zirconia
Characterization of cobalt dispersed on the mixed nanoscale alumina and zirconia supports, 352
$ZrO_2$
Synthesis and characterization of zirconia- and silica-doped zirconia nanopowders by oxalate processing, 315
$ZrO_2$–$SiO_2$
Synthesis and characterization of zirconia- and silica-doped zirconia nanopowders by oxalate processing, 315